Richter, P. H., & Eigen, M. (1974) *Biophys. Chem. 2*, 255–263.
Riggs, A. D., & Bourgeois, S. (1968) *J. Mol. Biol. 34*, 361–364.
Riggs, A. D., Bourgeois, S., & Cohn, M. (1970a) *J. Mol. Biol. 53*, 401–417.
Riggs, A. D., Suzuki, H., & Bourgeois, S. (1970b) *J. Mol. Biol. 48*, 67–83.
Riggs, A. D., Newby, R. F., & Bourgeois, S. (1970c) *J. Mol. Biol. 51*, 303–314.
Rosenberg, J. M., Kallai, O. B., Kopka, M. L., Dickerson, R. E., & Riggs, A. D. (1977) *Nucleic Acids Res. 4*, 567–572.
Sadler, J. R., Tecklenburg, M., & Betz, J. L. (1980) *Gene 8*, 279–300.
Shore, D., & Baldwin, R. L. (1983) *J. Mol. Biol. 170*, 957–981.
von Hippel, P. H., Revzin, A., Gross, C. A., & Wang, A. C. (1975) in *Protein–Ligand Interactions* (Sund, H., & Blauer, G., Eds.) pp 270–288, Walter de Gruyter, Berlin.
Wang, J. C., Barkley, M. D., & Bourgeois, S. (1974) *Nature (London) 251*, 247–249.
Whitson, P. A., Olson, J. S., & Matthews, K. S. (1986) *Biochemistry* (following paper in this issue).
Winter, R. B., & von Hippel, P. H. (1981) *Biochemistry 20*, 6948–6960.
Winter, R. B., Berg, O. G., & von Hippel, P. H. (1981) *Biochemistry 20*, 6961–6977.

Thermodynamic Analysis of the Lactose Repressor–Operator DNA Interaction†

Peggy A. Whitson, John S. Olson, and Kathleen Shive Matthews*
Department of Biochemistry, Rice University, Houston, Texas 77251
Received December 18, 1985; Revised Manuscript Received March 6, 1986

ABSTRACT: Kinetic and equilibrium constants for lactose repressor–operator DNA interaction have been examined as a function of salt concentration, size and sequence context of the operator DNA, and temperature. Significant salt effects were observed on kinetic and equilibrium parameters for pLA 322-8, an operator-containing derivative of pBR 322, and pIQ, an operator and pseudooperator-containing derivative of pBR 322. The association rate constant and equilibrium constant for the 40 base pair operator fragment were also salt dependent. Data for all the DNAs were consistent with a sliding mechanism for repressor–operator association/dissociation [Berg, O. G., & Blomberg, C. (1978) *Biophys. Chem. 8*, 271–280]. Calculation of the number of ionic interactions based on salt dependence yielded a value of ~8 for repressor binding to pIQ and pLA 322-8 vs. ~6 for the repressor–40 base pair fragment. These data and the differences in binding parameters for the plasmids vs. the 40 base pair operator are consistent with the formation of an intramolecular ternary complex in the plasmid DNAs. Unusual biphasic temperature dependence was observed in the equilibrium and dissociation rate constants for pLA 322-8, pIQ, and the 40 base pair fragment. These observations coupled with a discontinuity found in the inducer association rate constant as a function of temperature suggest a structural change in the protein. The large positive entropy contributions associated with repressor binding to all the DNAs examined provide the significant driving force for the reaction and are consistent with involvement of ionic and apolar interactions in complex formation.

The lactose repressor–operator DNA association rate is more rapid than three-dimensional diffusion would predict (Berg et al., 1981; Riggs et al., 1970). Protein translocation along the DNA has, therefore, been proposed to account for this facilitated association, in which the dimensionality of the search for the specific site is diminished; this movement has been postulated to consist primarily of sliding and/or intersegment transfer (Riggs et al., 1970; Richter & Eigen, 1974; Berg & Blomberg, 1976; Berg et al., 1981; von Hippel et al., 1975). Sliding is described as the one-dimensional protein movement along the DNA while nonspecific contacts are maintained. von Hippel et al. (1975) postulated intersegment transfer in which the protein is transiently bound between DNA segments; thus, translocation occurs as a series of random steps.

DNA has been modeled thermodynamically as a linear array of univalent negative charges [for review, see Lohman (1985)]. In a solution of a single salt, monovalent counterions may interact with the DNA by direct condensation, reducing the structural charge, or with the remaining bulk ions in solution, screening the phosphates of the DNA. Although the counterions condensed to the DNA are thought to be mobile, double-stranded DNA behaves thermodynamically as though 88% of its structural charge is neutralized in monovalent salts, independent of the salt concentration. When a protein binds to the DNA, it neutralizes some of the phosphates and consequently results in the release of counterions as well as affecting those counterions involved in screening. The repressor–operator DNA association is thermodynamically favored since the entropy of the system increases, due at least in part to release of ions from the DNA and the protein (Record et al., 1978).

Studies of the temperature dependence of the *lac* repressor–operator interaction have yielded limited information. Riggs et al. (1970) reported a 1.2-fold increase in the repressor–λ*plac* dissociation rate as temperature was increased from 1 to 37 °C and a 4-fold decrease in the association rate between 1 and 24 °C. Barkley et al. (1981) observed similar

† This work was supported by grants from the National Institutes of Health (GM-22441) and the Robert A. Welch Foundation (C-576).
* Author to whom correspondence should be addressed.

0006-2960/86/0425-3852$01.50/0

results for both the operator association and dissociation as a function of temperature. A biphasic temperature dependence for nonspecific DNA binding to repressor was reported by deHaseth et al. (1977). This paper compares previous kinetic and equilibrium results to those obtained by using alternate analytical methods for the rate determinations. Effects of salt, temperature, and size and sequence context of the operator DNA have been studied for the repressor–operator DNA interaction.

Materials and Methods

Isolation of Repressor. The lactose repressor was purified from *Escherichia coli* CSH 46 by the method of Rosenberg et al. (1977) as modified by O'Gorman et al. (1980). The purity of the repressor (>95%) was assessed by sodium dodecyl sulfate gel electrophoresis.

Assay of Repressor. Isopropyl β-D-thiogalactoside (IPTG)[1] binding activity was determined by the nitrocellulose filter and ammonium sulfate precipitation methods described by Bourgeois (1971). DNA binding assays using the nitrocellulose filter method were performed as described previously (Riggs et al., 1968; Hsieh & Matthews, 1981) with the modifications described in the previous paper (Whitson & Matthews, 1986). The buffer for DNA binding experiments, kinetic as well as equilibrium, was 0.01 M Tris-HCl, pH 7.4, 10^{-4} M DTT, 10^{-4} M EDTA, 5% dimethyl sulfoxide, and KCl at the indicated concentration (TFB). Bovine serum albumin (50 μg/mL) was added to this buffer to stabilize diluted protein (TBB). To minimize differences in buffer preparation, a 2 × stock of TFB was maintained; KCl was added to the appropriate concentration and the solution brought to twice the original volume. Since Tris-HCl buffers are susceptible to pH effects as a function of temperature, each buffer was equilibrated at the specified temperature prior to adjustment of the pH. Assays were carried out at the indicated temperature, maintained in an insulated waterbath controlled by a Brinkman Lauda K-2/RD circulating waterbath. Repressor concentrations represent total protein concentrations. The repressor protein was found to be 80–100% active from stoichiometry determinations.

Isolation and Labeling of Operator-Containing DNAs. Isolation and labeling of operator-containing DNAs was completed as described in the previous paper (Whitson & Matthews, 1986).

Measurement of Repressor–Operator Association Kinetics. Repressor–operator association kinetics were monitored as the time-dependent increase in the nitrocellulose filter-bound complex. DNA concentrations were 5.6×10^{-12} M for the 40 bp operator fragment and 4.4×10^{-13} M for pLA 322-8 and pIQ. Repressor concentrations ranged from 3×10^{-12} to 8×10^{-10} M in a total volume of 10 mL. An aliquot (0.4 mL) of the operator DNA in TBB was filtered before the repressor was added with mixing. Individual aliquots were filtered due to the small interval between time points. Reaction was monitored until equilibrium was attained (20 min), and nonspecific binding was determined by adding IPTG to 10^{-3} M. Analysis of these data is described under Results and Figure 1.

Measurement of Repressor–Operator Dissociation Kinetics. The lactose repressor protein was equilibrated with ^{32}P-labeled DNA in TBB of the indicated KCl concentration as described in the previous paper (Whitson & Matthews, 1986). The repressor–operator dissociation was monitored as the decrease in labeled, nitrocellulose filter-bound complex with time after the addition of an excess of unlabeled DNA. The actual equilibrium was determined and subtracted from each time point. The observed dissociation rate constant was then calculated from the $t_{1/2}$ by using $k_d = 0.693/t_{1/2}$.

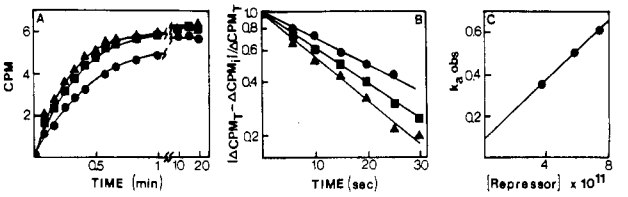

FIGURE 1: Determination of the bimolecular association rate constant of the 40 bp fragment. The observed association rate constant was obtained by monitoring the increase in filter-bound repressor–operator complex with time. Operator fragment (4×10^{-12} M) was equilibrated in 0.15 M KCl TBB at 25 °C; an aliquot was filtered before the addition of repressor and subsequently at the desired times until equilibrium was reached. Nonspecific binding was determined by adding IPTG to 10^{-3} M, and this value was subtracted from each point. (A) A real time course of the formation of the repressor–operator complex. (●) [Repressor] = 4.0×10^{-11} M; (■) [repressor] = 5.4×10^{-11} M; (▲) [repressor] = 7.2×10^{-11} M. (B) A normalized time course of the observed association rate constant. The y axis, $(\Delta cpm_{total} - \Delta cpm_i)/\Delta cpm_{total}$, represents the change in cpm relative to the equilibrium (total) change. The observed k_a can be determined from the time at which the reaction is 50% complete in (B), or from the slope of the line. The symbols and [repressor] are equivalent to (A). (C) Determination of the bimolecular association rate constant from a plot of the observed k_a vs. [repressor]. The slope of this plot (9.9×10^8 M^{-1} s^{-1}) represents the bimolecular association rate constant for the 40 bp fragment to repressor in 0.15 M KCl TBB.

Measurement of Inducer Association Rates as a Function of Temperature. A Gibson–Durrum rapid mixing stopped-flow spectrometer was used to measure the repressor–inducer association rate constants as a function of temperature. The excitation wavelength was 285 nm, and fluorescence emission at wavelengths greater than 350 nm was monitored. Pseudo-first-order conditions, in which repressor was 2×10^{-6} M and IPTG was 2×10^{-4} M before mixing, were used to measure the bimolecular association rate from the decrease in total fluorescence. Temperatures were maintained by a Brinkman Lauda K-2/RD circulating waterbath. Kinetic traces were fit to a single-exponential expression by using a linear least-squares algorithm (Bevington, 1969).

Quantitation of DNA. DNA was quantitated by absorbance at 260 nm ($A_{260}^{1\%} = 20$) and 0.1% ethidium bromide fluorescence as described by Le Pecq and Paoletti (1966). Fluorescence measurements were made on an SLM-400 spectrofluorometer by using an excitation wavelength of 546 nm and an emission wavelength of 590 nm. Calf thymus DNA was used as the standard.

Results

Repressor–Operator Association Kinetics. Association rates for the repressor–operator complex were measured as the increase in labeled operator–repressor complex bound to nitrocellulose with time. The bimolecular rate constant was measured directly under pseudo-first-order conditions, where repressor concentrations were at least 10-fold above the operator concentration. Figure 1A illustrates the exponential increase in labeled operator–repressor complex with time at the indicated repressor concentrations. Analysis of these data was simplified by plotting the $(\Delta cpm_{total} - \Delta cpm_i)/\Delta cpm_{total}$ after subtracting the nonspecific DNA binding, determined by adding IPTG to the reaction mixture (Figure 1B). The bimolecular association rate constant was calculated from the slope of a plot of the observed rate vs. repressor concentration

[1] Abbreviations: bp, base pair; DTT, dithiothreitol; EDTA, ethylenediaminetetraacetic acid; IPTG, isopropyl β-D-thiogalactoside; Tris-HCl, tris(hydroxymethyl)aminomethane hydrochloride.

Table I: Effects of Salt Concentration on the Kinetics and Equilibrium Binding of Repressor to 40 bp Fragment, pLA 322-8, or pIQ[a]

[KCl] (M)		40 bp	pLA 322-8	pIQ
0.150	k_a (M^{-1} s^{-1})	9.0×10^8	2.5×10^9	3.4×10^9
	k_d (s^{-1})	9.3×10^{-3}	2.1×10^{-3}	5.8×10^{-4}
	K_{dcalcd} (M)	1.0×10^{-11}	0.8×10^{-12}	1.8×10^{-13}
	K_{dobsd} (M)	1.0×10^{-11}	1.4×10^{-12}	5.0×10^{-13}
0.250	k_a (M^{-1} s^{-1})	2.2×10^8	2.5×10^8	3.0×10^8
	k_d (s^{-1})	1.7×10^{-2}	1.9×10^{-2}	2.1×10^{-3}
	K_{dcalcd} (M)	0.8×10^{-10}	7.6×10^{-11}	0.7×10^{-11}
	K_{dobsd} (M)	1.3×10^{-10}	7.1×10^{-11}	1.4×10^{-11}

[a] $K_{dcalcd} = k_d/k_a$.

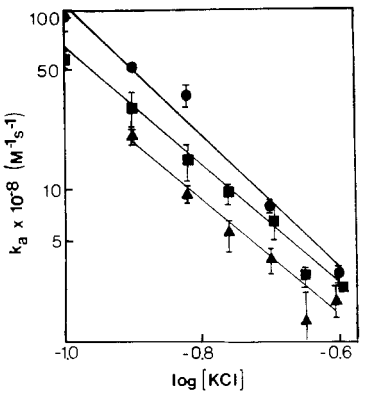

FIGURE 2: Effects of salt on the bimolecular association rate constant for pIQ, pLA 322-8, and the 40 bp fragment. Bimolecular association rate constants were determined as described in Figure 1 and under Materials and Methods for each salt concentration. Error bars indicate the standard deviation for 3–12 separate rate determinations at the indicated salt concentration at 25 °C. Lines represent the least-squares fit to the data. (●) pIQ; (■) pLA 322-8; (▲) 40 bp fragment.

(Figure 1C). The range of usable repressor concentrations was narrow and limited by large errors at both extremes. In 0.15 M KCl at 25 °C, the association rate constant of repressor–operator complex formation was 2.5 (±0.35) × 10^9 M^{-1} s^{-1} for pLA 322–8, 9.0 (±1.4) × 10^8 M^{-1} s^{-1} for 40 bp operator fragment, and 3.4 (±0.50) × 10^9 M^{-1} s^{-1} for pIQ (Table I).

Repressor–Operator Equilibrium Measurements. The equilibrium constants for repressor–operator DNA binding to 40 bp fragment, pLA 322-8, and pIQ were determined by nitrocellulose filter binding assays as described under Materials and Methods. Double-reciprocal plots of cpm vs. repressor concentration were used to calculate the observed binding constants from these equilibrium titrations. The K_d for the 40 bp operator fragment was 1.0 (±0.15) × 10^{-11} M in 0.15 M KCl TBB at 25 °C. The values measured for pLA 322–8 and pIQ in the same buffer were 1.4 (±0.40) × 10^{-12} M and 5.0 (±0.72) × 10^{-13} M, respectively. The increased affinity observed for pIQ indicates a potential function of pseudooperators in the binding process (Table I).

Salt Effects on Repressor–Operator Association and Equilibrium. The salt dependence of the repressor–operator DNA interaction was measured by varying the KCl concentration from 0.1 to 0.25 M. Both kinetic and equilibrium measurements were made by using these conditions for the 40 bp operator, pLA 322–8, and pIQ. The association rates decreased approximately 15-fold over the indicated KCl concentrations for all sizes of operator DNA (Figure 2). Association rates for pIQ were higher at all salt concentrations relative to either pLA 322–8 or the 40 bp fragment, and the association rates of pLA 322-8 were greater than for the 40 bp fragment.

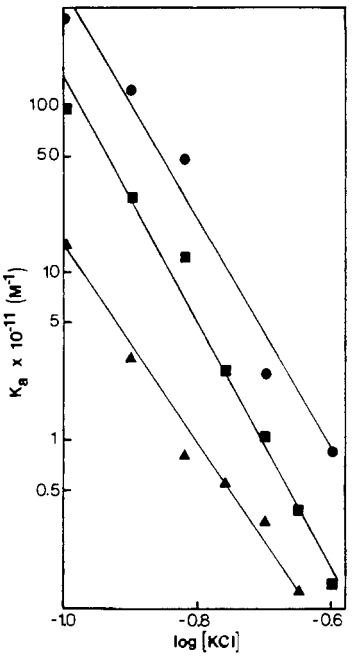

FIGURE 3: Effects of salt on equilibrium binding of repressor to pIQ, pLA 322-8 and the 40 bp fragment. K_a values were determined by k_a/k_d at 25 °C and plotted as a function of salt concentration. Lines represent the least-squares fit to the data. The slope of the line corresponds to counterions released, which can be equated to ionic interactions as described under Results. (●) pIQ; (■) pLA 322-8; (▲) 40 bp fragment.

Table II: Salt Dependence of the Kinetic and Equilibrium Parameters for the Repressor–Operator Interaction

DNA	$\partial \log k_a/\partial \log [K^+]$	$\partial \log k_d/\partial \log [K^+]$[a]	$\partial \log K_a/\partial \log [K^+] = -Z\psi$[b]	Z
40 bp fragment	3.5	0.69[c]	5.6 ± 0.14	6.4 ± 0.15
pLA 322-8	3.6	3.4[d]	7.3 ± 0.15	8.2 ± 0.17
pIQ	3.9	2.9[e]	7.0 ± 0.22	7.9 ± 0.25

[a] From the preceding paper (Whitson & Matthews, 1986). [b] ψ = 0.88. [c] Least-squares fit of data between 0.1 and 0.2 M KCl. [d] Least-squares fit of data between 0.1 and 0.225 M KCl. [e] Least-squares fit of data between 0.1 and 0.4 M KCl.

Equilibrium binding also exhibited a large KCl dependence (Table I and Figure 3). The equilibrium association constant for pIQ decreased approximately 100-fold as KCl concentration was increased from 0.1 to 0.2 M. The observed equilibrium binding constant was in good agreement with that calculated from the kinetic rate constants (k_d/k_a; Table I) except for pIQ and to a lesser extent pLA 322-8, at low salt concentrations (≤0.125 M). This behavior has also been reported for λ*plac* at low salt concentrations (Winter et al., 1981). The influence of size and sequence context of the operator DNA on the magnitude of the equilibrium constants (K_a) was similar to effects observed on the association rates, pIQ > pLA 322-8 > 40 bp fragment (Table I and Figures 2 and 3). The slope of a plot of log K_a vs. log [KCl] has been shown theoretically to be equivalent to the number of counterions released upon binding (Record et al., 1977, 1978; deHaseth et al., 1977; Barkley et al., 1981); this value can be equated to the ionic interactions by using the following equation: $\partial \log K_a/\partial \log [M^+] = -Z\psi$ = the number of counterions released, where ψ = 0.88 for double-stranded DNA, Z = number of ionic interactions, and $[M^+] = [K^+]$. The linearized plasmid DNAs, pIQ and pLA 322-8, had 7.9 ± 0.25 and 8.2 ± 0.17 ionic interactions involved in repressor binding, respectively, while the 40 bp operator fragment had

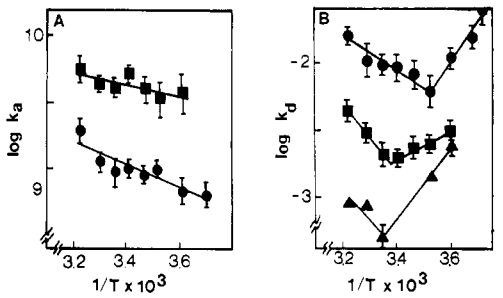

FIGURE 4: Arrhenius plots for the association and dissociation of repressor and operator DNAs. (A) The bimolecular association rates were measured at the indicated temperatures as described in Figure 1 and under Materials and Methods. (●) 40 bp operator fragment; (■) pLA 322-8. (B) Dissociation rates were obtained as described under Results and the previous paper (Whitson & Matthews, 1986). (●) 40 bp fragment; (■) pLA 322-8; (▲) pIQ.

Table III: Kinetic Thermodynamic Parameters for Repressor Interaction with the 40 bp Fragment or pLA 322-8

	E_a[a] (kcal/mol)	E_d[a] (kcal/mol)	A_a[b] (M^{-1} s^{-1})	A_d[b] (M^{-1} s^{-1})
40 bp fragment ($T \geq 10$ °C)	4.0	6.8	1.0×10^{12}	1.0×10^{3}
40 bp fragment ($T < 10$ °C)	4.0	−14.7	1.0×10^{12}	2.5×10^{-14}
pLA 322-8 ($T \geq 25$ °C)	2.0	10.9	1.3×10^{11}	2.0×10^{5}
pLA 322-8 ($T < 25$ °C)	2.0	−4.2	1.3×10^{11}	1.6×10^{-6}

[a] E = −(slope)2.303R of log k vs. $1/T$. [b] A = antilog (intercept) of log k vs. $1/T$.

Table IV: Equilibrium Thermodynamic Parameters for Repressor Interaction with the 40 bp Fragment or pLA 322-8

	ΔH[a] (kcal/mol)	ΔS[b] (cal/mol)	ΔG[c] (kcal/mol)
40 bp fragment ($T \geq 10$ °C)	−3.1	40	−15
40 bp fragment ($T < 10$ °C)	16	108	−14
pLA 322-8 ($T \geq 25$ °C)	−6.8	34	−17
pLA 322-8 ($T < 25$ °C)	6.6	82	−16

[a] ΔH = −(slope)2.303R of log K_a vs. $1/T$. [b] $\Delta S = (\Delta H - \Delta G)/T$. [c] $\Delta G = -RT \ln K_a$.

only 6.4 ± 0.15 ionic interactions (Table II).

Effects of Temperature on Repressor–Operator DNA Binding. The association and dissociation kinetics and the equilibrium DNA binding were measured for the 40 bp fragment and pLA 322-8 as a function of temperature (Figures 4 and 5). Arrhenius plots for both the association and dissociation rate constants were used to calculate the activation energy (Figure 4). From Figure 4, an activation energy of 4.0 kcal/mol for association of the 40 bp operator was determined, while the activation energy for pLA 322-8 association was 2.0 kcal/mol (Table III). While these plots for the association rate constants were linear, dissociation rate constants for the 40 bp operator, pLA 322-8, and pIQ were discontinuous when plotted in the same manner (Figure 4B). The activation energies for the dissociation reaction of the 40 bp operator ($T \geq 10$ °C), pLA 322-8 ($T \geq 25$ °C), and pIQ ($T \geq 25$ °C) were 6.8, 10.9, and 2.0 kcal/mol, respectively (Table III). Negative activation energies were observed for the dissociation process at low temperatures (Table III). From the slope of a plot of log K_a vs. $1/T$, ΔH can be determined (Figure 5; Table IV); the ΔG and ΔS values were calculated by using the equations indicated in Table IV. Figure 6 illustrates the enthalpy, entropy, and free energy changes for the course of the repressor–operator complex formation at

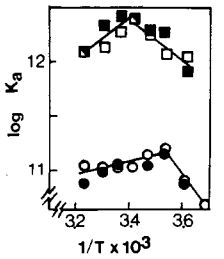

FIGURE 5: Temperature dependence of equilibrium repressor binding to operator DNA. A plot of log K_a vs. $1/T$ results in a slope equivalent to $-(\Delta H/RT)$. Values of ΔH are listed in Table IV. Open symbols represent K_a calculated from k_a/k_d, and closed symbols represent K_a observed by direct measurement of equilibrium binding. (●, ○) 40 bp fragment; (■, □) pLA 322-8.

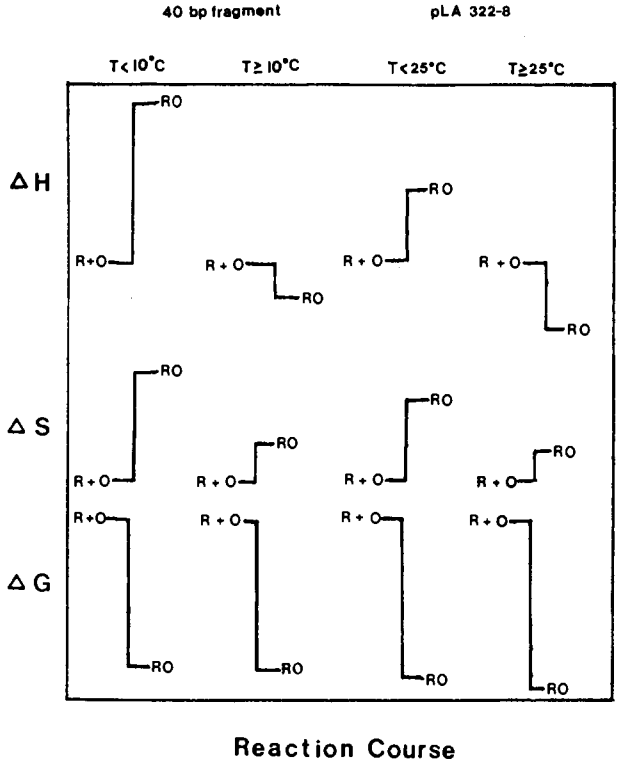

FIGURE 6: Enthalpy, entropy, and free energy reaction profiles for the 40 bp fragment and pLA 322-8 binding to repressor. R represents the repressor, O the operator, either the 40 bp fragment or pLA 322-8, and RO the repressor–operator complex. Entropy and free energy determinations were determined for $T = 298$ K or $T = 277$ K, above and below the inflection, respectively.

temperatures above and below the transition points. Activation enthalpies, entropies, and free energies were calculated from the kinetic data, assuming the Eyring theory, and the differences between the values for the forward and reverse reactions corresponded well to the observed equilibrium values.

Effects of Temperature on Repressor–IPTG Binding. To determine whether the discontinuity evident in DNA binding also affected repressor binding to inducer, repressor–IPTG association rate constants were monitored by stopped-flow fluorescence spectroscopy. An Arrhenius plot of the association rate constant resulted in a biphasic temperature dependence with an inflection at 12 °C (Figure 7). The activation energies were 0.52 (>12 °C) and 2.0 kcal/mol (<12 °C). These data provide additional evidence for a temperature-dependent structural change in the protein.

DISCUSSION

Effects of salt on the kinetics and equilibrium of repressor–operator DNA interactions have been studied previously

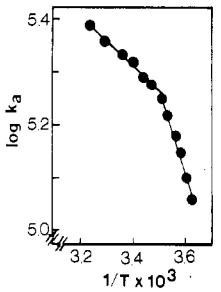

FIGURE 7: Arrhenius plot of inducer binding to the *lac* repressor. The inducer association rate constants were measured in 0.12 M potassium phosphate, pH 7.4, 10^{-4} M DTT, and 10^{-4} M EDTA as described under Materials and Methods.

(Barkley, 1981; Barkley et al., 1981; deHaseth et al., 1977; Record et al., 1977; Revzin & von Hippel, 1977; Winter & von Hippel, 1981; Winter et al., 1981). Protein binding to a polynucleotide results in the neutralization of a number of phosphates on the DNA molecule by cationic residues on the protein. The counterions condensed to the phosphates and the protein are released in solution upon binding, resulting in a salt dependence of this interaction (Lohman, 1985).

The presence of pseudooperator sequences resulted in an increased association rate (pIQ vs. pLA 322-8), although the absolute values we observed for the association rates for pIQ (a linearized ~6200 bp plasmid) were slightly lower between 0.1 and 0.2 M KCl than those obtained by Winter et al. (1981) by using an ~6700 bp fragment with pseudooperator sequences. The salt dependence of the association rate constant for pLA 322-8 (~4600 bp) most closely resembled data obtained for a 203 bp pseudooperator and operator-containing fragment (Winter et al., 1981). The comparable association rate constants for pLA 322-8 and the Hae-203 bp fragment of Winter et al. (1981) may be explained by an increase in the association rate constant for the shorter fragment due to the presence of the pseudooperators. The dependence of the association rate for the 40 bp operator fragment was diminished relative to the larger DNAs at all salt concentrations.

Measured equilibrium constants for the repressor–operator complex agreed well with those calculated from the rate constants (k_d/k_a), except for pIQ and, to a lesser extent, pLA 322-8 at low salt concentrations. As observed by Winter et al. (1981), kinetic measurements were found to have smaller standard deviations than direct determinations of equilibrium binding. Plots of the log of the calculated K_a vs. log [KCl] were used to determine that the repressor–operator DNA interaction involved approximately eight ionic interactions at 25 °C for pIQ and pLA 322-8 as compared to six to seven ionic interactions for λ*plac*, the 6700 bp fragment, and the Hae-203 bp fragment reported by Winter et al. (1981). The measurement of approximately six ionic interactions for the 40 bp operator (vs. approximately eight for pIQ and pLA 322-8) indicates that repressor–operator interactions extend beyond the central 40 bp of the operator region and/or that repressor binding to small DNA fragments is thermodynamically different than binding to larger DNA fragments. These differences may be ascribed to an increase in ionic interactions due to ternary complex formation for the larger DNAs, or alternatively the mechanism of repressor binding may not be the same for all DNAs.

Lohman et al. (1978) mathematically modeled two reaction mechanisms for protein–DNA interactions, screening controlled (one-step process) and preequilibrium (protein–DNA intermediate at equilibrium with the reactants). The salt dependence of the association and dissociation reactions has been used to distinguish between these two mechanisms (Lohman, 1985). In a screening-controlled reaction, the magnitude of $\partial \log k_d/\partial \log [K^+]$ is larger than that of $\partial \log k_a/\partial \log [K^+]$. If $\partial \log k_a/\partial \log [K^+] > \partial \log k_d/\partial \log [K^+]$ and $\partial \log k_d/\partial \log [K^+] < \partial \log K_a/\partial \log [K^+]$, a multistep process is indicated; thus, our data are consistent with a mechanism involving an intermediate for all the DNAs examined (Table II). Lohman et al. (1978), using the data of Goeddel et al. (1977), suggested that small operator fragments (26 and 21 bp) may be an example of a screening-controlled association of DNA and protein. In this case, a single-step mechanism applies, and the k_d is predicted to be more dependent on ionic strength than the k_a. In contrast, our association rates for the 40 bp operator were very salt dependent, while the dissociation rate was much less dependent on KCl concentration. The salt dependence of the association rate of the 40 bp fragment was of the same magnitude as that observed for pLA 322-8 and pIQ (Figure 2 and Table II). Even though the association rate data for the 40 bp fragment are similar to those obtained with pLA 322-8 and pIQ and suggest a multistep mechanism, the difference between $\partial \log k_d/\partial \log [K^+]$ and $\partial \log k_a/\partial \log [K^+]$ for the 40 bp fragment is inconsistent with predictions for either a steady-state preequilibrium model or a screening-controlled process as predicted by Lohman et al. (1978). This inconsistency may be ascribed to the inability of this small fragment to achieve a preequilibrium; that is, the intermediate in binding to this short DNA cannot be in equilibrium with the reactants. Thus, the assumptions for the derivation of the preequilibrium are not valid. It appears, however, that even binding to the 40 bp operator involves multiple steps, as this process cannot be described by a screening-controlled mechanism.

Berg and co-workers (Berg & Blomberg, 1976, 1977, 1978; Berg et al., 1981) have derived expressions for the association rate constant and dissociation rate constant assuming a two-step process for DNA binding:

$$R + D + O \rightleftharpoons RD + O \rightleftharpoons RO + D$$

where R = repressor, O = operator DNA, and D = nonspecific DNA. In this mechanism, a nonspecific complex is formed that facilitates the location of the operator site by the repressor. By use of a sliding model for the translocation process, the dependence of k_a on ion concentration derives primarily from K_{RD} [$k_a \propto (K_{RD})^{1/2}$] at higher salt concentrations (>0.1 M). The salt dependence of association would thus be expected to be approximately half that for K_{RD} (Berg et al., 1981; Barkley, 1981; Lohman, 1985). The values observed (Table II) are somewhat lower than those calculated on this basis (~3.5–4 vs. 5). The dissociation rate constant is predicted for sliding to be proportional to $K_{RD}^{1/2}/K_{RO}$, and the salt dependence will be $\partial \log k_d/\partial \log [M^+] = {}^1/_2\, \partial \log K_{RD}/\partial \log [M^+] - \partial \log K_{RO}/\partial \log [M^+]$ (Berg et al. 1981; Lohman, 1985). This relationship is realized for all three DNA species examined in this study (Whitson & Matthews, 1986). Thus, the salt dependences of the association and dissociation rate constants are consistent with sliding as a facilitative mechanism for locating the operator site.

Our kinetic and equilibrium data for the multiple repressor–operator interactions examined on different DNAs indicate a more complex mechanism for repressor binding to the operator is required to account for the differences observed between the DNA species. Formation of a ternary complex of operator–repressor–DNA may be invoked as a possible explanation for the smaller dissociation rate constants measured for the plasmid DNAs relative to the 40 bp operator (Whitson & Matthews, 1986). This mechanism would include a step

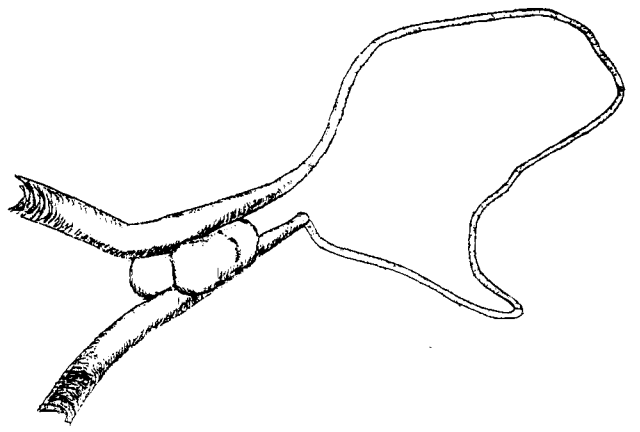

FIGURE 8: Schematic diagram of the ternary complex formation of operator–repressor–DNA (RO*). Both DNA binding sites of the repressor are occupied, and a looped DNA structure is formed. This diagram illustrates DNA binding through the long axis of the protein as proposed by Dunaway et al. (1980), though ternary complex formation could occur with the DNA aligned along the short axis of the protein.

for the formation of an intramolecular ternary complex between the operator sequence, bound repressor, and another sequence of DNA (nonspecific or pseudooperator; Figure 8):

$$RO \overset{K^*}{\rightleftharpoons} RO^*$$

where R = repressor, O = operator DNA, RO* = the intramolecular ternary complex, and K^* = equilibrium constant for the intramolecular step. When the filter-binding technique is used, RO and RO* are not distinguishable; however, their presence can be ascertained by the effects of salt concentration and size and sequence context of the operator-containing DNAs. At equilibrium, under the conditions of our assays, RO and RO* would be expected to be the predominant species. Assuming minimal difference in the repressor–operator interaction (RO) for each of the DNAs, the observed K_a for the 40 bp fragment would correspond to the K_a for RO formation (K_{RO}), since an intramolecular ternary complex cannot be formed with this fragment. The observed K_a for larger DNAs would be equal to $K_{RO}(1 + K^*)$. Assuming K_{RO} for operator in the larger piece of DNA is equal to that observed directly for the 40 bp fragment, K^* for pLA 322-8 with an operator–repressor–nonspecific DNA complex can be computed to be $\sim$12 at 0.15 M KCl. The effective concentration of nonspecific DNA sites in the DNA domain surrounding the repressor–operator complex may be estimated from the length (4600 bp) as $\sim 2 \times 10^{-4}$ M bp (Shore & Baldwin, 1983). Assuming $K^* \sim 10$ (0.1 M KCl), an intramolecular binding constant for nonspecific DNA binding to the repressor–operator can be calculated as $\sim 5 \times 10^4$ M^{-1}. Fried and Crothers (1984), using a gel electrophoretic technique, reported a K_m of $\sim 2.5 \times 10^{-5}$ M for operator dissociation initiated by adding nonspecific DNA. In their ternary complex model, this value corresponds to an equilibrium constant for nonspecific DNA binding to the repressor–operator complex of $\sim 4 \times 10^4$ M^{-1} (0.05 M NaCl). This value, obtained from a very different experimental approach, correlates very well with that calculated by assuming an intramolecular ternary complex. The differences in salt conditions for the two measurements will minimally influence this calculation since the K^* value does not change dramatically with salt ($K^* \sim 10$ at 0.1 M KCl vs. 12 at 0.15 M KCl). The observed K_a for pIQ would include the K^* for operator–repressor–pseudooperator formation. Again, assuming the same value of K_{RO} applies, K^* for pIQ is $\sim$55 (0.15 M KCl) and indicates that even more RO* is formed in the presence of pseudooperator sequences. The effective local concentration for pseudooperators relative to repressor bound to operator is $\sim 10^{-7}$ M; thus, $K^* = 55$ can be converted to a pseudooperator binding constant to the repressor–operator complex of $\sim 10^9$ M^{-1}. In both cases, the presence of intramolecular DNA binding sites greatly stabilizes the operator DNA complex.

If the plasmid DNAs are presumed to include (1) a primary site equivalent to the 40 bp operator and (2) a second site for nonspecific or pseudooperator DNA, the difference in Z values for these DNAs can be interpreted as an estimate for the ionic interactions present at the second site. This value is $\sim$2 and is notably lower than the corresponding parameter for the presumed primary site ($\sim$6). Whether this difference reflects a different type of complex formation between protein and DNA at the second site or other factors that influence the binding is not apparent. At high salt concentrations (>0.25 M), the formation of ternary complex (i.e., occupation of the second site by nonspecific DNA) would be unfavorable as K^* is somewhat salt dependent, and the 40 bp operator and operator-containing plasmid DNA would be expected to behave similarly, as we have observed for the dissociation rate constant (Whitson & Matthews, 1986).

Previous temperature studies of the *lac* repressor–operator DNA binding showed only slight temperature effects on the association and dissociation rate constants. Mossing and Record (1985) have observed equilibrium enthalpy changes for the *lac* repressor–operator interaction of 14 (±5) kcal/mol between 5 and 23 °C, and Riggs et al. (1970) reported a value of 8.5 kcal/mol. We observed a smaller ΔH of 6.6 kcal/mol for repressor binding to pLA 322-8 over the same temperature range. Interestingly, the temperature dependence of the equilibrium constant was discontinuous for pLA 322-8, pIQ, and the 40 bp fragment and correlated to similar nonlinear behavior of the dissociation rate constant. In contrast, the temperature dependence of the association rate constant for repressor binding to pLA 322-8 and the 40 bp fragment was linear. Since the rate-limiting steps for operator DNA association are probably diffusion to the nonspecific DNA and sliding to the operator site, a temperature effect on specific repressor–operator interactions would not be observed. However, a structural change in the protein affecting the specific release of the repressor from the operator would be evident in the dissociation rate constants.

The equilibrium constant for nonspecific DNA binding has also been reported to be temperature dependent (deHaseth et al., 1977), with a similar point of discontinuity as repressor binding to pLA 322-8. The high temperature protein structure has a higher specific/nonspecific equilibrium DNA binding ratio than the lower temperature structure. Thus, nonspecific DNA would compete for repressor binding more effectively at low temperatures. Association rate constants for IPTG binding to repressor, monitored by using stopped-flow fluorescence techniques, also demonstrated a biphasic temperature dependence (inflection 12 °C); these data in combination with those observed for DNA binding suggest a temperature-dependent protein structural change. The point of inflection varies with the DNA or sugar ligand, indicating that the bound ligand may modulate the structural state of the protein. Sugar modulation of subunit dissociation has been observed by using high hydrostatic pressure to dissociate the repressor (Royer et al., unpublished observations).

Repressor binding to the 40 bp fragment and pLA 322-8 is favored entropically. Positive entropies are thought to be

the result of solvent and/or structural effects (Laidler & Peterman, 1979). Charge neutralization and hydrophobic interactions result in a release of counterions and solvent molecules and a corresponding gain of entropy. Also, a more open conformation of a molecule allows more freedom of movement and, therefore, results in increased entropy. The large salt effects on the repressor–operator interaction confirm that charge neutralization contributes to the overall increase in entropy. Hydrophobic interactions may also play a significant role in effecting the large entropic factor in binding (Cantor & Schimmel, 1980). From the energy diagram (Figure 6), the 40 bp fragment and pLA 322-8 appear to bind repressor similarly at high and low temperatures. Binding enthalpy is more favorable for pLA 322-8 than the 40 bp fragment at high temperatures. Decreasing the temperature below the point of discontinuity results in a dramatic increase in the entropy contribution for both DNAs. The entropy effects at all temperatures for both DNAs are favorable for repressor binding, as might be expected from the large number of counterions released; however, operator binding to the lower temperature structure is clearly more favorable in terms of entropy changes. The large increase in ΔS at low temperatures is unusual, and it is noted that this increase almost precisely balances a significant unfavorable change in enthalpy to maintain an almost constant value for ΔG.

In conclusion, data reported here indicate approximately two fewer ionic interactions for the 40 bp operator ($Z \simeq 6$) than for pIQ and pLA 322-8 ($Z \simeq 8$), suggesting either that ionic contacts may extend beyond the 40 bp operator region or, as indicated by other data, that ternary complex formation increases the number of ionic contacts. From the thermodynamic parameters, interactions of repressor and the 40 bp operator or pLA 322-8 appeared generally similar. An apparent structural change in the repressor was observed with different transition temperatures depending on the size and sequence context of the DNA studied and on the sugar ligand. The structural change appeared to affect primarily the dissociation rate of the repressor–operator DNA complex. This temperature-dependent structural transition of the protein resulted in an increase in the enthalpic requirement for DNA binding and a corresponding increase in the entropy change with minimal alteration in the free energy for the interaction.

ACKNOWLEDGMENTS

We thank J. A. Gardner and W. R. Light for data analysis programs and Dr. T. Lohman for critical reading of the manuscript and helpful discussions.

REFERENCES

Barkley, M. D. (1981) *Biochemistry 20*, 3833–3842.

Barkley, M. D., Lewis, P. A., & Sullivan, G. E. (1981) *Biochemistry 20*, 3842–3851.

Berg, O. G., & Blomberg, C. (1976) *Biophys. Chem. 4*, 367–381.

Berg, O. G., & Blomberg, C. (1977) *Biophys. Chem. 7*, 33–39.

Berg, O. G., & Blomberg, C. (1978) *Biophys. Chem. 8*, 271–280.

Berg, O. G., Winter, R. B., & von Hippel, P. H. (1981) *Biochemistry 20*, 6929–6948.

Bevington, P. R. (1969) in *Data Reduction and Error Analysis for the Physical Sciences*, McGraw-Hill, New York.

Bourgeois, S. (1971) *Methods Enzymol. 21D*, 491–500.

Cantor, C. R., & Schimmel, P. R. (1980) in *Biophysical Chemistry: The Conformation of Biological Macromolecules* (Bartlett, A. C., Ed.) pp 287–288, W. H. Freeman, San Francisco.

deHaseth, P. L., Lohman, T. M., & Record, M. T., Jr. (1977) *Biochemistry 16*, 4783–4791.

Dunaway, M., Manly, S. P., & Matthews, K. S. (1980) *Proc. Natl. Acad. Sci. U.S.A. 77*, 7181–7185.

Fried, M. G., & Crothers, D. M. (1984) *J. Mol. Biol. 172*, 263–282.

Goeddel, D. V., Yansura, D. G., & Caruthers, M. H. (1977) *Proc. Natl. Acad. Sci. U.S.A. 74*, 3292–3296.

Hsieh, W.-T., & Matthews, K. S. (1981) *J. Biol. Chem. 256*, 4856–4862.

Laidler, K. J., & Peterman, B. F. (1979) *Methods Enzymol. 63*, 234–257.

Le Pecq, J.-B., & Paoletti, C. (1966) *Anal. Biochem. 17*, 100–107.

Lohman, T. M. (1985) *CRC Crit. Rev. Biochem. 19*, 191–245.

Lohman, T. M., deHaseth, P. L., & Record, M. T., Jr. (1978) *Biophys. Chem. 8*, 281–294.

Mossing, M. C., & Record, M. T., Jr. (1985) *J. Mol. Biol. 186*, 295–306.

O'Gorman, R. B., Dunaway, M., & Matthews, K. S. (1980) *J. Biol. Chem. 255*, 10100–10106.

Record, M. T., deHaseth, P. L., & Lohman, T. M. (1977) *Biochemistry 22*, 4791–4796.

Record, M. T., Anderson, C. F., & Lohman, T. M. (1978) *Q. Rev. Biophys. 11*, 103–178.

Revzin, A., & von Hippel, P. H. (1977) *Biochemistry 16*, 4769–4776.

Richter, P. H., & Eigen, M. (1974) *Biophys. Chem. 2*, 255–263.

Riggs, A. D., Bourgeois, S., Newby, R. F., & Cohn, M. (1968) *J. Mol. Biol. 34*, 365–368.

Riggs, A. D., Bourgeois, S., & Cohn, M. (1970) *J. Mol. Biol. 53*, 401–417.

Rosenberg, J. M., Kallai, O. B., Kopka, M. L., Dickerson, R. E., & Riggs, A. D. (1977) *Nucleic Acids Res. 4*, 567–572.

von Hippel, P. H., Revzin, A., Gross, C. A., & Wang, A. C. (1975) in *Protein–Ligand Interactions* (Sund, H., & Blauer, G., Eds.) pp 270–288, Walter deGruyter, Berlin.

Whitson, P. A., & Matthews, K. S. (1986) *Biochemistry* (preceding paper in this issue).

Winter, R. B., & von Hippel, P. H. (1981) *Biochemistry 20*, 6948–6960.

Winter, R. B., Berg, O. G., & von Hippel, P. H. (1981) *Biochemistry 20*, 6961–6977.